

## ORIGINAL ARTICLE

Medicine Science 2022;11(2):869-76

## 2.45 GHz electromagnetic radiation hazard on the rat cortical femur: morphometric and biomechanical evaluations

 Aysegul Akar<sup>1</sup>,  Murat Erdem Gultiken<sup>2</sup>,  Durmus Bolat<sup>3</sup>,  Neslihan Ormanci<sup>4</sup>,  
 Begum Korunur Engiz<sup>5</sup>,  Ertugrul Sunan<sup>6</sup>,  Ulku Comelekoglu<sup>7</sup>

<sup>1</sup>Ondokuz Mayıs University, Faculty of Medicine, Department of Biophysics, Samsun, Turkey

<sup>2</sup>Ondokuz Mayıs University, Faculty of Veterinary, Department of Anatomy, Samsun, Turkey

<sup>3</sup>Kırıkkale University, Faculty of Veterinary, Department of Anatomy, Kırıkkale, Turkey

<sup>4</sup>Samsun Veterinary Control and Research Institute, Samsun, Turkey

<sup>5</sup>Ondokuz Mayıs University, Faculty of Engineering, Department of Electrical and Electronics Engineering, Samsun, Turkey

<sup>6</sup>Samsun University Veterinary Control and Research Institute, Samsun, Turkey

<sup>7</sup>Mersin University Faculty of Medicine, Department of Biophysics, Mersin, Turkey

Received 30 December 2021; Accepted 22 February 2022

Available online 27.04.2022 with doi: 10.5455/medscience.2021.12.419

Copyright@Author(s) - Available online at [www.medicinescience.org](http://www.medicinescience.org)

Content of this journal is licensed under a Creative Commons Attribution-NonCommercial 4.0 International License.



### Abstract

We aimed to investigate the positive or negative biological effects of Microwave (MW) exposure on rat femur by morphometric analysis and biomechanical test methods. 22 adult rats were separated into two groups: Group first was used as the control group and the second group of rats was used as a study group which was subjected with 2.45 GHz MW frequency for two hours a day for 21 days. Both groups were sacrificed for morphometric and biomechanical evaluation at the end of 21 days. Morphometric properties were measured using Stereo investigator analyzing system programs. In biomechanical measurements, the femurs of control and exposed group rats were evaluated by intrinsic and extrinsic biomechanics properties. Biomechanical measurements were performed from the left femur mid-diaphysis using a three-point bending test. In the morphometrically measurements, significant differences were statistically found ( $p < 0.05$ ). Biomechanically, there was also a change in extrinsic and intrinsic biomechanics properties between the two groups ( $p < 0.05$ ). This study shows that non-ionizing radiation exposure at a low-level electric field (about 12 V/m, 0.079W/kg) in 2.45 GHz MW radiation might cause morphological and biomechanics alterations on mechanical properties in the rat cortical femur.

**Keywords:** Low-level electric field, 2.45GHz, Microwave radiation; bone, biomechanical properties, stereo investigator

### Introduction

The modern telecommunication devices used such as laptop computer, wireless and Bluetooth, base station and mobile phone system (such as 2G,3G,4.5G) and medical devices used for diagnosis and treatment such as thermal therapy, Radiofrequency (RF) ablation, and Magnetic resonance imaging (MRI) emitting RF or/and Microwave (MW) have brought disadvantages as well as advantages to our natural life in daily life. The frequencies used in MW communication are usually in the range of 2 to 2.45 GHz with low power levels [1,2]. When low level or high-level electric field emitted from MW devices faced with a biological system, it could cause thermal and/or non-thermal effects.

Specific Absorption Rate (SAR) used to evaluate absorbed dose in the biological system of RF or MW exposure is a dosimetric value suggested by considering thermal effects by Organizer institutions such as American National Standards Institute-ANSI, National Council on Radiation Protection-NCRP and International Commission Non-Ionizing Radiation Protection-ICNIRP. It has been discussed thermal and/or non-thermal effect mechanisms of RF and MW exposure on different tissues or all bodies in the reports and some articles in detail [3-6]. This unexplained effect mechanism has still being discussed. An important point associated with the mechanism is the coupling of electric fields and their distribution inside the body. In general, coupling into the body of the electric field in high frequency is stronger than the magnetic field [2]. Because of coupling into the body at high frequency, it is reported that currents along the legs and torso at electric field exposure, absorption is maximum at limbs with the percentage of 70% of the power absorbed in the body, especially for MW exposure [2]. For this reason, it is important to investigate

\*Corresponding Author: Aysegul Akar, Ondokuz Mayıs University, Faculty of Medicine, Department of Biophysics, Samsun, Turkey  
E-mail: [aysegula@omu.edu.tr](mailto:aysegula@omu.edu.tr)

MW exposure of bone.

The bone has mechanical functions such as providing support to the body, role-playing to transfer forces as a lever system, protecting the internal organs and in addition, it has physiological properties such as forming blood cells and depositing calcium [7]. Bone is very important for life as it is a component of the skeletal system that protects, supports, and moves the body. The mechanical properties of the bone are an important term that indicates the functional property of the bone. Biomechanical tests are frequently used in pathological conditions, treatment, and diagnostic methods. Therefore, investigation of its morphological or structural aspects is vital to determine the quality of bone. Physical properties such as mass, length, area, volume, and areal moment of inertia of the bone require morphometric data of biological structures, and computer-supported image analyzing programs have been used to obtain these data. In the last decade, morphometric properties of biological structures are obtained by using image analyzing systems such as the Stereo investigator workstation imaging system. Stereo investigator workstation imaging system is sophisticated computerized microscope control created to obtain estimates of morphometric properties of any biological structure. The advantage of this device is that the software and hardware work in harmony. In addition, the Stereo investigator workstation has also supplied advances in some research such as human placenta morphometry, hippocampal morphometry, and surface area of the kidney [8-10].

The biological effects of ionizing or/and non-ionizing radiation or a toxic substance on the biomechanics of bone were the focus of attention by most researchers [11-15] and the negative effects of ionizing radiation on bone biomechanics have also been declared by some researchers [11,16,18-20] and reviews [21,22]. Nevertheless, there are many reports and researches on the positive effects of low and/or high-frequency non-ionizing radiation such as bone healing, wound healing, tumor therapy, and ion transitions at the cellular level [13,14,23-25]. However, the positive or negative effects of High Frequency-Electromagnetic field (HF-EMF) non-ionizing radiation on bone biomechanics are not clear and there are a few studies and the investigations have still gone on HF-EMF. We aimed to investigate the positive or negative biological effects of MW exposure at low-level electric fields used frequently daily on femur by morphometric analysis and biomechanical test methods.

## Materials and Methods

### Establishment of Working Groups

This study was performed on male Wistar rats (8-12 weeks old) obtained from the Veterinary Control and Research Institute Ethics Committee, Samsun (SVKEYEK/2011-04). A total of 22 rats were used in the study and the experimental animals were separated into 2 groups containing equal numbers of rats the groups were formed as follows;

Group I (Control group): The animals in this group were fed with standard rat chow and not exposed to any EMF.

Group II (Exposed group): In addition to the animals in this group fed with standard rat chow, exposed in 2.45 GHz MW, about 12 V/m, 0.079W/kg, (2 hours a day for 21 days). Each of the rats was

weighed at the beginning and the end of the study (Table 1). The rats were euthanized at the end of the study. Their femurs were subjected order to morphological and biomechanical evaluations. Control and exposed cortical femur specimens were stored at -20°C wrapped in gauze soaked with isotonic solution [26].

**Table 1.** Average weights of the rats before and after study

	Control Group	Exposed Group	P-value
<b>Initial mean weight (g)</b>	382.4±20	368.0±35	0.308 (p>0.05)*
<b>Post mean weight (g)</b>	380.6±20	357.5 ±30	0.074 (p>0.05)*

All data are expressed as means ± SD. \*Weight between Group 1 and group 2 was evaluated with a t-test

### Microwave exposure system and application

In this study, a 2004X-RF (Set Electronic Co, Adapazarı, Turkey) microwave generator was used to generate MW at a frequency of 2-2.45 GHz. Before the study, the background of electric field and magnetic field in the laboratory were detected by the Electrical and Electronic Engineering Department at the Ondokuz Mayıs University via PMM 8053 electric field meter. PMM 8053 Portable Field Meter can perform instant measurements at X, Y, Z Cartesian coordinates and time axis, and, the EP-330 electric field probe with 0.3 V/m- 300 V/m level range can measure at 100 kHz-3 GHz frequency range. Because of the level range of the electric field and magnetic field devices background electric field and magnetic field lower than 0.3 V/m and 0.8mA/m were not detected in the experimental medium. The exposure application of rats has shown in Figure 1. Here, a galvanized plate with 1 mm thick was placed for grounding of the static field at the bottom of a pie cage plexiglas restrainer (50x20x7cm). The distance between antenna and galvanized plate was about 15 cm and the coaxial cable-rat distance in the horizontal position was about 6 cm.

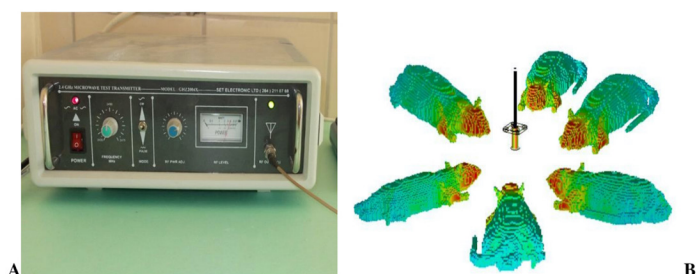


**Figure 1.** Microwave exposure system and application. A. Model: 2004X-RF microwave generator, B. Monopole antenna, and rat exposure

### E-field measurements, E- field distributions, and Specific absorption rate (SAR) Calculation

In this study, the rats were placed to a single 12-slices pie cage restrainer the ventilation was provided with a 2 cm diameter hole at the top. 2004XRF signal generator's output power was set to 0.4 W to get about 12 V/m average E-field (Eavg). Regularly every week, E-field levels were measured at the head, dorsal, and tail of each rat from the top surface of the pie cage restrainer by PMM 8053 Portable Field Meter. The 33 total (Eavg) data were saved on a computer for further evaluation. By calculating the means of each rat's head, torsal, and tail Eavg values, a whole-body Eavg value was obtained. The total 33 whole body Eavg values at the

end of 3 weeks were calculated in SPSS 15 and were expressed as means  $\pm$  standard deviations (SD). The whole-body Eavg value for the 11 rats for 21 days was  $11.96 \pm 0.89$  V/m. This data ( $11.96 \pm 0.89$  V/m) was referenced to evaluate the E-field distribution in the pie cage restrainer and the rat and, to determine SAR distribution through the electromagnetic simulator.

Non-ionizing radiation dosimeter has a significant role to assess the risk of human exposure to MW radiation, e.g., electric field distribution, evaluation of SAR. However, measurement of E-field distribution inside the body directly is rarely possible. Various numerical analysis techniques are available such as finite-difference method (FDM), finite element method (FEM), Finite Integration Technique (FIT), and FDTD which are used for electromagnetic field assessments. The FIT is a discretization method for Maxwell's integral equations, and it allows performing numerical simulations using resulted matrix equations of the discretized fields. In this study, E-field distribution and SAR for 10 gr of tissue on the rats were calculated through simulations using CST Microwave Studio 2018. The experimental setup was transferred to a simulation environment which consists of a monopole antenna and voxel rat models, and then E-field distribution and SAR calculations were completed. In the simulations, perfect boundary approximation, the hexahedral mesh type was used, and the 10g averaged SAR in the rat was calculated according to IEEE/IEC 62704-1 averaging method. E-field and SAR distributions were shown in Figure 2 A and B, respectively. It can be seen from Figure 2. B that 10g average SAR level of the whole body is 0.0719 W/kg.

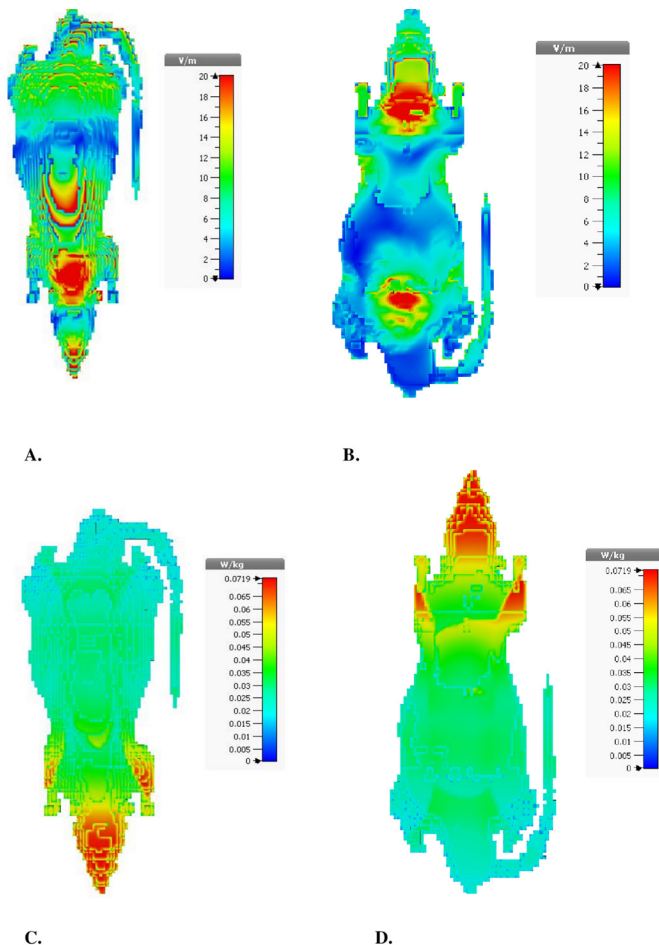


**Figure 2.** Distribution of E-Field (Top view A, B) and SAR over 10 grams of tissue (Bottom view C, D)

## Morphometric and biomechanical evaluations

In this study, the cortical femur samples stored at  $-20^{\circ}\text{C}$  were brought to room temperature and soft tissue from the samples was removed for morphometrically and biomechanical evaluations. Both control and exposed group femurs were also divided randomly into two groups. The femurs in the first group (5 left 6 rights, total 11 femurs) were used for morphometric evaluation. The femurs (6 left, 5 right, total 11 femurs) in the second other were calculated using a three-point bending test to determine bone biomechanical properties.

## Morphometric evaluations

In this study, the muscle and other tissues on the right and left femurs of the control and exposed group were dissected. The femur mass and length were measured with a precision balance instrument (Presica Model LS 220A, SCS, Labomar, Switzerland) and a Mitutoyo Digital Caliper (Model CD-15D, Mitutoyo Corporation, Kawasaki, Japan), respectively. For morphometric evaluations, each femur was cut approximately 2 mm thick with a Proxon MiniMot 40 hand saw (Proxon GmbH Inc Spanischen 18-24 DE-54518 Niersbach Rheinland-Pfalz, Germany) and 12-16 sections were obtained from each femur. At the morphometric evaluation, it was evaluated femur mass, length, and Anteroposterior (AP) cortical thickness, Mediolateral (ML) cortical thickness, inside and outside radius of bending cortical area, and areal moment of inertia of bending cortical area, bending cortical area of femur, cortical area, and volumes of the femur, total area and volume of the femur. The obtained sections were photographed with the Olympus C-5060 (Olympus America Inc., Melville, New York, USA) to measure morphometric parameters by the Stereo investigator workstation imaging system. The arithmetic mean of the cross-sectional areas passing through the femur corpus was considered to be the femur bending cortical area. While the femur cortical area was calculated, the sections taken from the proximal and distal epiphyses were excluded from the calculation. To determine the areal moment of inertia and to make precise measurements, the mediolateral outside radius ( $X_1$ ), the mediolateral inside radius ( $X_2$ ), the anteroposterior outside radius ( $Y_1$ ), the anteroposterior inside radius ( $Y_2$ ), the bending cortical area, the cortical area and volume of the femur, the medullary area and the volume of the femur, the total area, and volume of the femur were determined with Stereo investigator image analysis system consisting of (Leica® DM4000, Leica Microsystems CMS GMBH, Wetzlar, Germany), a computer-controlled three-axis stage (Ludl Mac 5000®; Ludl Electronic Products Ltd, New York), a digital camera (MBF® 2000R Fast 1394 Color; Qimaging, Surrey, Canada) and stereology software (Stereo investigator®; MBF Bioscience, Williston, VT). The calculation of cortical and medullary cross-sectional surface areas of each femoral section in the Stereo investigator by point counting method have shown in Figure 3. The green dots in the corresponding section represent the cortical areas and the yellow dots represent the medullary areas. To keep the Coefficient Error (CE) value of the study below 0.05, the distance between the two points was determined as  $400\text{ }\mu\text{m}$  and at least 250 points fell in the relevant regions were calculated for the volume estimation of the cortical and medullary regions in each femur. The cortical and medullary volumes for each femur were estimated using the formula  $V=txa$  according to Cavalieri's method. Where  $V$ =volume,  $t$ =slice thickness, and  $a$ , is the area on



the cross-section of the relevant structure. Cavalieri's method, one of the stereological methods, was used to measure the volume of subcomponents of the femur (Figure 3). The femur morphometric properties have given in Table 2.



**Figure 3.** The calculation of cortical and medullary area using Stereo investigator. Cross-sectional moment of inertia (mm<sup>4</sup>) or the areal moment of inertia was calculated from equation [27]

$$I(mm^4) = \frac{3.14}{64} (X_1 Y_1^3 - X_2 Y_2^3)$$

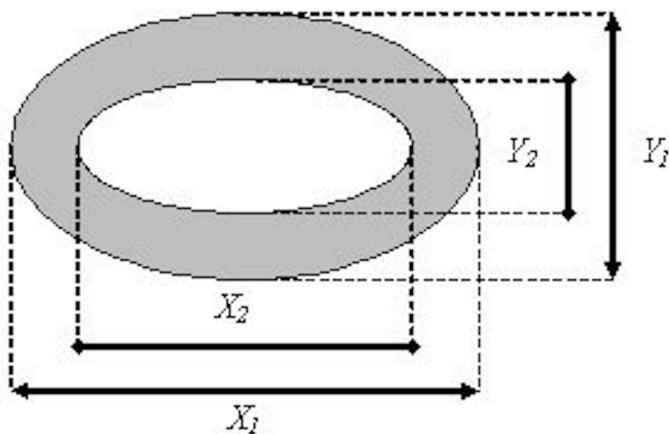


**Figure 4.** X1 is the mediolateral outside radius, X2 is the mediolateral inside radius, Y1 is the anteroposterior outside radius. Y2 is the anteroposterior inside radius (This figure was adapted from An and Draughn 1999) [27]

## Biomechanical evaluation

### Biomechanical test application

The second group of femurs (6 left and 5 rights, a total of 11 femurs) was evaluated using a three-point bending test to determine biomechanical properties of the cortical bone. The three-point bending test application was made at room temperature using an Instron Universal test instrument (Lloyd LRX, Lloyd Instruments Ltd., Fareham, Hants United Kingdom (Figure 5)). The procedures of the bending test were set as performed by Bozzini et al., (2009) [28]. The bending test application to measure biomechanical properties of the samples was applied on mid-diaphysis of the femur placed horizontally as shown in Figure 5. Ringer's solution was applied to prevent drying during the testing of the femurs. The three-point bending test was performed to measure intrinsic and extrinsic properties determining the biomechanical properties of

cortical femurs. The three-point bending speed of the device was set 5 mm/min in all tests. Distance between the two ends was 13-15 mm (Figure 5). After biomechanics test application, the load-deformation curves were obtained for group 1 and group 2 (Figure 6A, B). This graph was used to obtain extrinsic biomechanical properties, ultimate load (N), elastic limit (N), deformation (mm), stiffness (N/mm), and energy absorption capacity (EAC-N.mm).

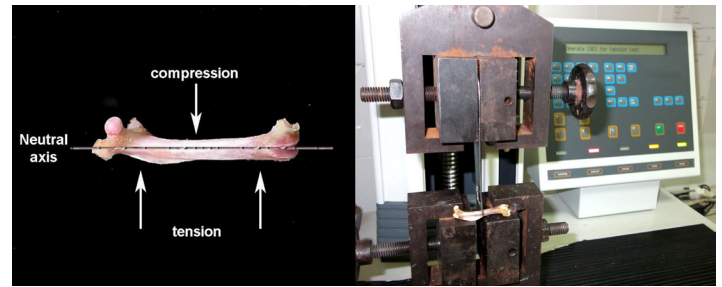


**Figure 5.** Three-point bending application for biomechanical tests-Lloyd LRX, Lloyd Instruments Ltd., Fareham, Hants United Kingdom

The ultimate load was determined from the maximum load that the material has sustained before failure in the load-deformation curve (Figure 6A). The elastic limit was calculated from the load at the yielding point. The deformation was specified from the transverse deformation at the point of loading. Stiffness was described from the slope of the linear region of the load-deformation graph (N/mm). The area under the load-deformation graph was indicated as EAC and this parameter is defined as the energy (work to failure; U) stored by the bone until it breaks and provides information about the fragility of the bone. The load-deformation data to determine intrinsic properties of cortical femur were recorded at BIOPAC-MP100 Acquisition System Version 3.5.7 and the load-deformation recording was normalized by bending cortical area. These curves were converted to a stress-strain graph and this curve was generated for each cortical femur. Stress, strain, young module, and toughness were achieved from this graph. The stress (N/mm<sup>2</sup>) was calculated by dividing the ultimate load to the bending cortical area. The strain was calculated as the deformation of the sample divided by the initial gauge length (in mm/mm). The area under the stress-strain graph was defined as toughness (N/mm<sup>2</sup>). An elastic module or young module which expresses the intrinsic stiffness of the tissue was evaluated from the slope of the linear region of the stress-strain graph [27,29].

### Statistical analysis

Statistical calculations were made using the Student t-test in JASP statistical analysis program for morphometric evaluations. SPSS statistical package version 15.0 was used for biomechanical evaluations and Npar test was performed for normally distributed data and statistical analysis was made using a two-sample t-test to examine differences between the groups. All results were given as mean±standard deviation (SD) and median (minimum-maximum). The significance level was set at p<0.05 and the p-value less than 0.05 and 0.001 were considered as statistically significant.

## Results

### Morphometrically properties of the femur in control and exposed groups

Table 1 shows the comparison between the weight of both groups before and after the study. There were no statistical before and

after from the study between group I and group II. Although not statistically significant, there is a post-study change in the weight of the exposed group, group II (3.54%).

Table 2 lists the geometric properties of the rat femur. For excepted femur mass and femur length, AP and ML cortical thickness, the mediolateral outside radius-X1, the mediolateral inside radius-X2, the anterior-posterior outside radius-Y1, and the anterior-posterior inside radius-Y2 were measured by Stereo investigator and the areal moment of inertia was calculated from this data. Femur mass, the Y1 radius, and the areal moment of inertia were significant, decreased in exposed rats ( $p<0.001$ ). There were no statistically change between the control and MW exposed group concerning rat femur length, the X1 radius, the X2 radius, and the Y2 radius ( $p>0.05$ ). While AP cortical thickness was significantly decreased in the exposed group compared to that of the controls, ( $p<0.01$ ), ML cortical thickness of the exposed group was not statistically different from control. It was also evaluated bending cortical area, cortical area and volume of the femur, medullary area and volume of the femur, total area, and total volume of the femur using Stereo investigator. It was found that except for the medullary area of the femur, femur areas (bending cortical area, cortical area of femur, total area of femur) were significantly different than that of the control rats by 26%, 37.1%, and 28.3%, respectively ( $p<0.05$ ). Except for femur cortical volume, also no significant differences were observed between the two groups at the medullary, and the total volume of the femurs was estimated from all groups ( $p>0.05$ ).

**Table 2.** Geometrical and Morphometrical values

		Control Group (n=11)	Exposed Group (n=11)	P value
Femur mass (g)		1.15±0.06	0.980±0.8	<0.001
Femur length (mm)		40.0313±0.27	39.28±0.95	0.184
AP cortical thickness (μm)		0.7810±0.074	0.6826±0.068	0.0097**
ML cortical thickness (μm)		0.8271±0.107	0.8596±0.010	0.5136
X <sub>1</sub> (mm)		4.163±0.510	4.351±0.289	0.336
X <sub>2</sub> (mm)		2.509±0.340	2.631±0.214	0.3639
Y <sup>1</sup> (mm)		3.612±0.298	3.269±0.220	0.0127*
Y <sup>2</sup> (mm)		2.050±0.215	1.903±0.164	0.1212
I (mm <sup>4</sup> )		8.698±2.359	6.628±1.152	0.019*
Femur area (mm <sup>2</sup> )	Bending cortical area	9.743±3.21	7.205±0.92	0.022*
	Cortical area of the femur	148.6±62.67	93.46±13.21	0.0104*
	Medullary area of the femur	74.31±10.97	66.34±15.75	p>0
	The total area of the femur	222.9±63.49	159.8±26.32	0.0075**
Femur volume (mm <sup>3</sup> )	Cortical volume of femur	326.1±36.54	278.5±26.01	0.0032**
	The medullary volume of the femur	196.9±35.05	184.2±32.23	p>0
	Total volume of femur	510.3±57.38	475.5±48.98	p>0

Mean±SD,  $p<0.05$ ,  $p<0.001$ . All values are given mean±SD in tabular form, SD= Standard Deviation, \*represents statistical significance, \*\* represents strong significance

Mechanical parameters of the femur in control and exposed groups

Table 3 shows intrinsic and extrinsic biomechanical properties of the femurs. Extrinsic properties were found from the load-deformation curve and intrinsic properties were evaluated from the stress-strain curve. Biomechanically, ultimate load, elastic limit, deformation, stiffness, EAC, strain, toughness, and young module from extrinsic and intrinsic biomechanical properties of the rat femurs were found to be different between the control and study groups.

**Table 3.** Biomechanical properties of the rat cortical femurs

		Control Group (n=11)	Exposed Group (n=11)	P
Extrinsic properties	Ultimate load (Breaking force (N))	120.531±19.253	101.3618±11.427	0.013
	Elastic limit (N)	102.5 ± 11.28	82.8 ± 9.12	0.005
	Deformation (mm)	1.3844±0.218	0.9618±0.196	<0.001
	Stiffness (N/mm)	84.19±12.01	114.16±16.19	0.002
	Energy absorbed capacity (N.mm)	83.2588±17.44	48.5870±10.779	<0.001
Intrinsic properties	Stress (N/mm²)	12.987±2.739	14.211±1.884	0.252
	Strain (%)	0.0369±0.0057	0.0245±0.00477	<0.001
	Toughness (N/mm²)	0.2402±0.0669	0.1759±0.0481	0.022
	Young modules (N/mm²)	359.52±95.084	593.668±103.33	<0.001

Mean±SD,  $p<0.05$ , \* $p<0.001$

Mean maximum load was decreased in exposed group rats (15.9%) compared to that of the controls ( $P<0.05$ , Figure 6A and 7A). The elastic limit was lower than that of the control rats by 19.2% ( $P<0.05$ , Figure 6B and 7B). Deformation was significantly decreased in exposed group rats by 30.5% ( $P<0.001$ , Figure 6 and 7C).

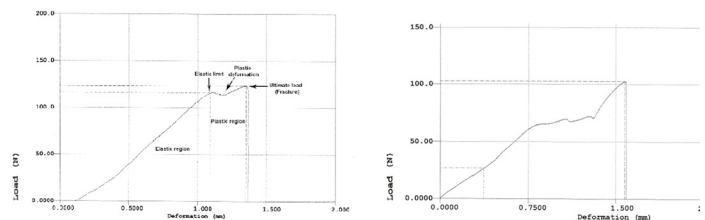


**Figure 6.** Load-deformation curve, A: for control group and B: exposed group

Stiffness values of the femurs of exposed group rats were different in exposed rats, 35.6%, from that in controls and there was statistically significant ( $P<0.05$ , Figure 7D). Femurs of exposed group rats had less absorbed energy (41.6%) than that in controls ( $p<0.001$ , Figure 7E).

The intrinsic parameters have given in table 3. The stress, strain, toughness, and young module parameters, which are related to the material phase of the bone, were found to change by 9.4%, 33.6% ( $p<0.001$ , Figure 7F), 26.7% ( $p<0.05$ , Figure 7G) and 65.1% ( $p<0.001$ , Figure 7H) in MW exposed rats compared to control

rats, respectively.

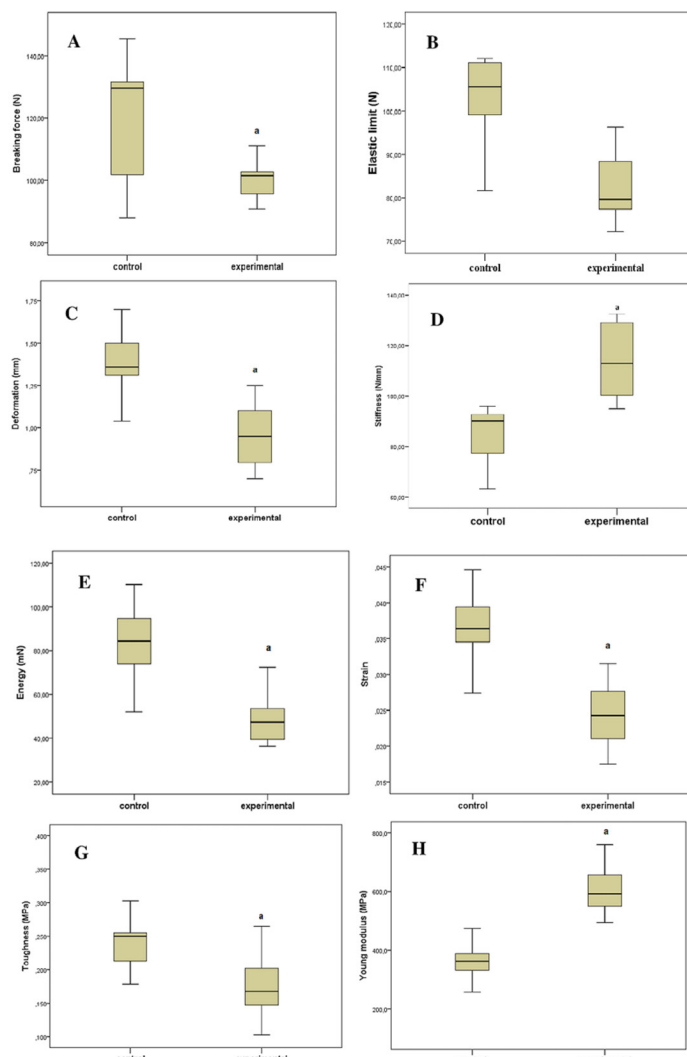


**Figure 7.** Bone biomechanics parameters of rats' femurs. A, B, C, D and E, F, G, H are shown rats' femur extrinsic and intrinsic biomechanics results, respectively.  $p < 0.05$ ;  $p < 0.001$ ; exposed group compared to control. The cases where statistically significant differences were found are given in the figure

## Discussion

In the present study, we investigated the positive or/and negative effects of short-term (for 21 days), 2.45 GHz  $11.96 \pm 0.89$  V/m, 0.0719 W/kg SAR, MW exposure on the biomechanics properties of the cortical femur using stereological methods and biomechanical methods. There are many studies investigating the positive and/or non-constructive effects of ionizing or non-ionizing radiation on the use of extremely low frequencies (approximately 50Hz) and high-frequency range on the bone. However, there are especially very few studies in low electric field limb exposure on the bone negative/or positive effects of RF and MW radiation used for data transmission and medical applications. However, in the ICNIRP 2020 report [30], it is recommended to focus on limbs in the new exposure limits and there are very few studies on limbs at low-level MW frequency. In current studies, it has been reported that mobile phone communication device has positive or negative effects on growth and/or adult bone development, fracture healing, structural changes, bone metabolism, mostly at frequencies of 900, 1800, 2100MHz via histological, morphological, radiological

and mineral density/or biomechanics. In a study, the effects on bone development in the prenatal period were investigated in rats exposed to 1800 MHz EMF for six, 12,24 hours/day for 20 days [31]. In conclusion, because of the histological and morphological evaluation, it was found that EMF might damage muscle, bone, and cartilage tissues in the prenatal period. NISBET et al., 2016 [32], evaluated the effects of 900 MHz and 1800 MHz EMF on the growth plate in rats growing 2 hours/day for 90 days. As a result of clinical, radiological, histopathological, and biochemical analyzes, they showed that EMF could cause prolongation of the growth process in growing rats. In another study, its effects on bone fracture healing were investigated at 900 MHz frequency for 30 minutes a day, 5 days a week for 8 weeks [13]. As a result, they showed that 900 MHz frequency negatively affects bone fracture healing. ASLAN et al.'s study by 2014 [14] found that 1800 MHz frequency at different frequency 2W output power, 30 minutes a day, 5 days a week, 8 weeks, and 0.008W/kg SAR did not affect bone fracture healing. In another study, they reported a positive effect of 2100 MHz frequency on bone fracture healing at 2W output power, 3 hours a day, 7 days a week for 28 days, and a maximum SAR value of 0.1W/kg [15]. Because of studies, it has also been reported that ionizing radiation affects bone tissue metabolism and biomechanical parameters negatively (especially from irradiation after 14 and 21 days) [20]. In our study, it was observed that non-ionizing radiation had negative effects on the cortical femur, in line with the studies performed.

The most important effect of radiation on bone is that it causes atrophy by reducing the number of components. This starts with vascular changes in the tissue and leads to negative effects on the production and preservation of the bone matrix [33]. Narrow Haversian canals affect the formation of sclerotic connective tissue within this space [34]. Studies have shown that radiation disrupts the balance between bone resorption and reduced mineralization and bone formation [35]. The decrease in the number of cells is associated with collagen production and decreased activity of alkaline phosphatase [36], which leads to decreased bone tissue mineralization and osteopenia [33]. The maximum load is the tensile force used biomechanically evaluated as bone and must be exerted to induce fracture. Stiffness and EAC are properties associated with the bone mineral component [12,29]. In our study, an increase in stiffness of rat femoral bone and a decrease in maximum load and EAC indicate a negative effect of non-ionizing radiation on bone strength. These findings are also consistent with previous studies [17,37,38].

Ultimate stress, strain, Young module, and toughness are important parameters in the evaluation of bone strength and they are known to be indicators of intrinsic parameters [29,39,40]. In biomechanical evaluation, stress, strain, Young module, and toughness parameters are parameters related to the mineral phase and collagen phase of bone tissue. An increase and/or decrease among these parameters may herald problems such as poorly mineralized bone, hyper mineralized bone, increased crystallinity, denaturation of the collagen molecule, deboning of mineral/collagen in bone tissue. In addition, it is reported that these changes in the tissue because of exposure of the bone to various undesirable stresses for any reason can also cause various diseases such as osteomalacia and osteomalacia [29,40]. In this study, the young module significantly increased, while toughness and strain were significantly reduced



in rats exposed with 2.45 GHz MW radiation alone compared to controls. However, there was no decrease or increase in the ultimate stress value. Non-ionizing radiation-induced reductions in general biomechanical parameters and morphometric measurements were demonstrated in this study. These reductions suggest that they are related to bone strength. These findings are consistent with the findings of a previous study by CURREY et al., (1997) [16].

The bone biomechanical parameters are related to both its geometrical or morphometric properties and the bone composition [12]. These parameters are important in evaluating the femur cross-sectional area or bending cortical area, cortical bone quality and strength [41-43]. The significant decrease in the exposed group (group 2) compared to the control group in our study is consistent with other studies. This supports the idea that non-ionizing radiation can also reduce bone strength. The main parameters that determine the structural behavior of bone (ie strength and fragility) in morphometric and biomechanical evaluation are the geometry of the bone (such as bone mass, length, thickness, area), the mass distribution of the bone (ie microarchitecture), and material properties. For example, measuring these properties provides information that the greater the cross-sectional area, the stronger the bone. In our study, bone mass, anterior-posterior cortical thickness of the bone, anterior-posterior outer radius, field moment of inertia, bent cortical area, cortical area, total area, bone structure-related medullary and total volume and geometry were significantly different in the exposed group compared to the control group. was found to be lower ( $p < 0.05$ ). These results show us that the strength of the bone structure of the exposed group is adversely affected by the 2.45 GHz frequency exposure, and also raises suspicion that there may be a change in its microarchitecture. However, although there was no significant difference in the age and weight of the study groups at the beginning of the study, it was observed that the weight of the exposed group tended to decrease after the study. The geometric properties of cortical bone are important as they reflect the bone's resistance to fracture. For this reason, the change in weight, structure and geometry of exposed rats compared to the control increases the thought that their bone metabolism is negatively affected.

## Conclusion

The results of this study indicate that non-ionizing radiation exposure at low level electric field (about 12 V/m, 0.079W/kg) in 2.45 GHz MW might cause morphological and biomechanics alterations on mechanical properties in the rat cortical femur. This result has been required further research using advanced research methods such as XRD and SEM-EDX.

## Acknowledgements

*A part of this study was presented in the Third ICLAS East Mediterranean Meeting and The XV ICLAS.*

## Conflict of interests

*The authors report no conflicts of interest. The authors alone are responsible for the content and writing of the paper.*

## Financial Disclosure

*The authors declare that they have received no financial support for the study.*

## Ethical approval

*This study was performed on male Wistar rats obtained from the Veterinary Control and Research Institute Ethics Committee, Samsun (SVKEYEK/2011-04).*

## Author contributions

*Aysegül Akar and Murat Erdem Gültiken conceived the experiments and designed the study. Neslihan Ormanci took care of the rat and conducted the 2.45GHz Microwave radiation exposure of rats. Background of electric field and magnetic field in the laboratory were detected and Weekly rat exposure electric field measurements were made by Ertuğrul Sunan and Aysegül Akar. Begüm Korunur Engiz calculated the SAR with CST programme. Morphometrical measurements and stereoinvestigator image analysis were conducted by Durmuş Bolat. Ülkü Çömelekoğlu conducted biomechanics analyzes. Aysegül Akar wrote the manuscript. All the authors reviewed the manuscript.*

## References

1. Independent Expert Group on Mobile Phones (IEGMP). Mobile Phones and Health (The Stewart Report), Report 1-167. <https://www.emf-portal.org/en/article/11173>. 2000
2. International Commission on Non-Ionizing Radiation Protection Exposure to high-frequency electromagnetic fields, biological effects and health consequences (100 kHz –300 GHz)–review of the scientific evidence and health consequences. 2009: <https://www.icnirp.org/en/publications/article/hf-review-2009.html>
3. Adair RK. Biophysical Limits on Athermal Effects of RF and Microwave Radiation. *Bioelectromagnetics*. 2003;24:9-48.
4. Belyaev I. Non-thermal Biological Effects of Microwaves. *Microwave Review*. 2005;11:13-29.
5. Foster KR, Glaser R. Thermal mechanisms of interaction of radiofrequency energy with biological systems with relevance to exposure guidelines. *Health Phys*. 2007;92:609-20.
6. Yakymenko I, Tsybulin O, Sidorik E, et al. Oxidative mechanisms of biological activity of low-intensity radiofrequency radiation. *Electromagn Biol Med*. 2016;35:186-202.
7. Nigg M, Herzog W. *Biomechanics of the Musculo-Skeletal System*, 2007. 3rd ed. Edited by BENNO, Chichester: John Wiley Sons.
8. Haeussner E, Schmitz C, Von Koch F, Frank Hg. Birth weight correlates with size but not shape of the normal human placenta. *Placenta*. 2013;34:574-82.
9. Gigliotti JC, Huang L, Ye H, Bajwa A, et al. Ultrasound Prevents Renal Ischemia-Reperfusion Injury by Stimulating the Splenic Cholinergic Anti-Inflammatory Pathway. *J Am Soc Nephrol*. 2013;24:1451-60.
10. Boschen K, Ruggiero MJ, Klintsova AY. Neonatal binge alcohol exposure increases microglial activation in the developing rat hippocampus. *Neuroscience*. 2016;324:355-66.
11. Comelekoglu U, Yalın S, Bagis S, et al. Low-exposure cadmium is more toxic on osteoporotic rat femoral bone: mechanical, biochemical, and histopathological evaluation. *Ecotoxicol Environ Saf*. 2007;66:267-71.
12. Gurgul S, Erdal N, Yılmaz SN, Yıldız A, Ankaralı H Deterioration of bone quality by long-term magnetic field with extremely low frequency in rats. *Bone*. 2008;42:74-80.
13. Aslan A, Atay T, Gulle K, et al. Effect of 900 MHz electromagnetic fields emitted from cellular phones on fracture healing: An experimental study on rats. *Acta Orthop Traumatol Turc*. 2013;47:273-80.
14. Aslan A, Kırdemir V, Kocak A, et al. Influence of 1800 MHz GSM-like Electromagnetic Radiation Exposure on Fracture Healing. *Arch Med Res*. 2014;45:125-31.
15. Durgun M, Dasdag S, Erbatur S, et al. Effect of 2100 MHz mobile phone radiation on healing of mandibular fractures: an experimental study in rabbits. *Biotechnol Biotechnological Equipment*. 2016;1:112-20.
16. Currey JD, Foreman J, Laketic I. Effects of ionizing radiation on the mechanical properties of human bone. *J Orthop Res*. 1997;1:111-7.
17. Zhou XZ, Zhang G, Dong QR. Low-dose X- irradiation promotes mineralization of fracture callus in a rat model. *Arch Orthop Trauma Surg*. 2009;129:125-32.
18. Barth HD, Zimmermann EA, Schaible E, et al. Characterization of the effects of X-ray irradiation on the hierarchical structure and mechanical properties of human cortical bone. *Biomaterials*. 2011;32:8892-904.
19. Demirel C, Kılıksız S, Gurgul S, et al. N-acetylcysteine ameliorates  $\gamma$ -radiation-induced deterioration of bone quality in the rat femur. *J Int Med Res*. 2011;39:2393-2401.

20. Soares PB, Soares FCJ, Limirio PHJO, et al. Effect of ionizing radiation after-therapy interval on bone: histomorphometric and biomechanical characteristics. *Clin Oral Investig*. 2019;23:2785-93.
21. Pacheco R, Stock H. Effects of Radiation on Bone. *Curr Osteoporos Rep*. 2013;11:299–304.
22. Zhang J, Qiu X, Xi K, et al. Therapeutic ionizing radiation induced bone loss: A review of in vivo and in vitro findings. *Connective Tissue Research*. 2018;59:509-22.
23. Ciombor DM, Aaron RK. The role of electrical stimulation in bone repair. *Foot Ankle Clin*. 2005;10:579-93.
24. Haddad JB, Obolensky AG, Shinnick P. The biologic effects and the therapeutic mechanism of action of electric and electromagnetic field stimulation on bone and cartilage: New findings and a review of earlier work. *J Altern Complement Med*. 2007;13:485-490.
25. Markov MS. Expanding Use of Pulsed Electromagnetic Field Therapies. *Electromagn Biol Med*. 2007;26:257-74.
26. Turner CH, Burr DB. Basic biomechanical measurements of bone: A Tutorial. *Bone*. 1993;14:595–608.
27. An, YH, Draughn RA. Mechanical Testing of Bone and the Bone-Implant Interface, 1st Ed., 1999, New York: CRC Press LLC.
28. Bozzini C, MI Olivera, Huygens P, et al. Long-term exposure to hypobaric hypoxia in rat affects femur cross-sectional geometry and bone tissue material properties. *Ann Anat*. 2009;191:212-7.
29. Turner CH. Biomechanics of bone: determinants of skeletal fragility and bone quality. *Osteoporos Int*. 2002;13:97-104.
30. International Commission on Non-Ionizing Radiation Protection (2020): ICNIRP guidelines for limiting exposure to electromagnetic fields (100 kHz to 300 GHz).<https://www.icnirp.org/cms/upload/publications/ICNIRPrfgdl2020.pdf>.
31. Erkut A, Tumkaya L, Balık MS, et al. The effect of prenatal exposure to 1800 MHz electromagnetic field on calcineurin and bone development in rats. *Acta Cir Bras*. 2016;31:74-83.
32. Nisbet HO, Akar A, Nisbet C, et al. Effects of electromagnetic field (1.8/0.9 GHz) exposure on growth plate in growing rats. *Res Vet Sci*. 201;104:24-9.
33. Ergun H, Howland WJ. Postradiation atrophy of mature bone. *CRC Crit Rev Diagn Imaging*. 1980;12:225-43.
34. Oest ME, Policastro CG, Mann KA, et al. Longitudinal effects of single hindlimb radiation therapy on bone strength and morphology at local and contralateral sites. *J Bone Mineral Res*. 2018;33:99-112.
35. Green DE, Rubin CT. Consequences of irradiation on bone and marrow phenotypes, and its relation to disruption of hematopoietic precursors. *Bone*. 2014;63:87-94.
36. Sams A. The effect of 2000r of X-rays on the acid and alkaline phosphatase of mouse tibiae. *Int J Radiat Biol Relat Stud Phys Chem Med*. 1966;10:123-40.
37. Maeda M, Bryant MH, Yamagata M, et al. Effects of irradiation on cortical bone and their time-related changes: a biomechanical and histomorphological study. *J Bone Joint Surg Am*. 1988;70:392-9.
38. Nyaruba MM, Yamamoto I, Kimura H. Bone fragility induced by X-ray irradiation in relation to cortical bone-mineral content. *Acta Radiol*. 1998; 39:43–46.
39. Reddy G, Stehno-Bittel L, Hamade S. The biomechanical integrity of bone in experimental diabetes. *Diabetes Res Clin Pract*. 2001;54:1-8.
40. Burr DB. The contribution of the organic matrix to bone's material properties. *Bone*. 2002;31:8-11.
41. Martin RB, Boardman DL. The effects of collagen fiber orientation, porosity, density and mineralization on bovine cortical bone bending properties. *J Biomech*. 1993;26:1047–54.
42. Ferretti JL, Cointy GR, Capozza RF. Analysis of biomechanical effect on bone and on the bone muscle interactions in small animal models. *J Musculoskelet Neuronal Interact*. 2001;1:263–74.
43. Ito M, Nishida A, Koga A. Contribution of trabecular and cortical components to the mechanical properties of bone and their regulating parameters. *Bone*. 2002;31:351-8.